

## Supporting Information

*for*

### **Core-shell metal-organic-framework (MOF)-based smart nanocomposite for efficient NIR/H<sub>2</sub>O<sub>2</sub>-responsive photodynamic therapy against hypoxic tumor cells**

*Hui-Juan Cai,<sup>a</sup> Ting-Ting Shen,<sup>a</sup> Jian Zhang,<sup>b</sup> Chang-Fu Shan,<sup>a</sup> Jian-Guo Jia,<sup>a</sup> Xiang Li,<sup>a</sup> Wei-Sheng Liu,<sup>a</sup> Yu Tang\*<sup>a</sup>*

<sup>a</sup> State Key Laboratory of Applied Organic Chemistry, Key Laboratory of Nonferrous Metal Chemistry and Resources Utilization of Gansu Province, College of Chemistry and Chemical Engineering, Lanzhou University, Lanzhou 730000, P. R. China.

<sup>b</sup> Department of Chemistry, University of Nebraska-Lincoln, Lincoln, NE 68588-0304, USA

## **Contents**

### **1. Experimental Section**

- 1.1 Materials and Instruments
- 1.2 Synthesis of Nanocomposites
- 1.3 Experimental Methods

### **2. Characterization Section**

- 2.1 . Dynamic Light Scattering (DLS)
- 2.2 . TEM Image of PVP-stabilized UCNPs
- 2.3 . TEM Image of UCNPs/MB@ZIF-8 (oleate-capped UCNPs)
- 2.4 . Elemental Mapping Images of UCNPs/MB@ZIF-8
- 2.5 . EDS of UCNPs@ZIF-8 and UCNPs/MB@ZIF-8
- 2.6 . Powder X-ray Diffraction (XRD) Patterns and N<sub>2</sub> Adsorption-desorption Isotherms
- 2.7 . Elemental Mapping Images and XPS of UCNPs/MB@ZIF-8@catalase

### **3. Spectroscopic Studies**

- 3.1 . UV-vis Spectra
- 3.2 . FTIR Spectra
- 3.3 . Fluorescence Spectra

### **4. Zeta Potential**

### **5. The Decay Curves**

### **6. The Oxygen-Generation Performance of UCNPs/MB@ZIF-8@catalase**

### **7. The Leakage of MB**

### **8. Cell Viability and Intracellular Generation of Singlet Oxygen**

### **9. Cell Death Imaging and In-vitro Confocal Microscope Images**

## 1. Experimental Section

### 1.1 Materials and Instruments

**Materials.** Yttrium chloride ( $\text{YCl}_3 \cdot 6\text{H}_2\text{O}$ ), ytterbium chloride ( $\text{YbCl}_3 \cdot 6\text{H}_2\text{O}$ ), and erbium chloride ( $\text{ErCl}_3 \cdot 6\text{H}_2\text{O}$ ) were prepared by reacting  $\text{Y}_2\text{O}_3$ ,  $\text{Yb}_2\text{O}_3$ , or  $\text{Er}_2\text{O}_3$  (99.99%, Shanghai Yuelong) with hydrochloric acid. Oleic acid (OA, >90%), and 1-octadecene (ODE, >90%) were purchased from Alfa Aesar. 2-Methylimidazole, polyvinylpyrrolidone (PVP,  $M_w=40,000$ ), 1,3-diphenylisobenzofuran (DPBF), methylene blue (MB), 3-aminopropyltriethoxysilane (APTES), catalase, and 1-(3-dimethylaminopropyl)-3-ethylcarbodiimide hydrochloride (EDC·HCl) were all purchased from J&K Scientific Ltd. Zinc nitrate ( $\text{Zn}(\text{NO}_3)_2 \cdot 6\text{H}_2\text{O}$ ), NaOH, and  $\text{NH}_4\text{F}$  were obtained from Tianjin Guangfu Technology Development Co., Ltd. (Tianjin, China). 3-[4,5-Dimethylthiazol-2-yl]-2,5-diphenyl tetrazolium bromide (MTT) was purchased from Solarbio Co., Ltd. Dulbecco's Modified Essential Medium (DMEM), fetal bovine serum (FBS), Ham's F12 (F12), and trypsin-EDTA solution were purchased from Gibco. 2,7-Dichlorofluoresceindiacetate (DCFH-DA) was bought from Biosearch Technologies Inc.

**Instruments.** Powder X-ray diffraction (PXRD) patterns were recorded over the  $2\theta$  range from 10 to  $70^\circ$  using a Rigaku-Dmax 2400 diffractometer with  $\text{Cu K}\alpha$  radiation. Fourier transform infrared (FTIR) spectra of the materials were conducted within the 4000 - 400  $\text{cm}^{-1}$  wavenumber range by using a Nicolet 360 FTIR spectrometer with the KBr pellet technique. Transmission electron microscopy (TEM) images were taken on a Tecnai-G2-F30 (300 kV). Inductively coupled plasma-atomic emission spectroscopy (ICP) was conducted using an IRIS Advantage ER/S spectrophotometer. The morphological, structural and chemical characterization of all samples were analyzed at the nano/atomic scale using field emission HRTEM (Tecnai™ G2 F30;

FEI Company, USA) working at 120 kV, which was equipped with EDX (AMETEK Inc., USA) and high-angle annular dark-field scanning transmission electron microscopy (HAADF-STEM). Dynamic light scattering (DLS) measurement was conducted on a Zetasizer Nanoseries (Nano ZS90) instrument. The UC emission spectra were acquired using a 980 nm laser as the irradiation source and detected by a PMT detector on the fluorescence instrument (FLSP920, Edinburgh instruments, the UK) from 450 to 700 nm. The instrument of UCLM was measured on an inverted fluorescence microscope (Olympus FV1000), and a 980 nm diode laser was illuminated. The measurements above were all performed at room temperature.

## 1.2 Synthesis of Nanocomposites

**Synthesis of NaYF<sub>4</sub>:60%Yb,2%Er NPs (abbreviated as UCNPs).** The  $\beta$ -phase NaYF<sub>4</sub>:Yb/Er NPs were synthesized via a co-precipitation method.<sup>S1</sup> A slightly modified procedure was used. YCl<sub>3</sub>·6H<sub>2</sub>O (0.38 mmol), YbCl<sub>3</sub>·6H<sub>2</sub>O (0.60 mmol), and ErCl<sub>3</sub>·6H<sub>2</sub>O (0.02 mmol) were dispersed in oleic acid (OA, 8 mL) and 1-octadecene (ODE, 15 mL), and then the mixture was heated to 160 °C for 1 h with a gentle flow of argon gas to obtain lanthanide-oleate precursors. After the formation of a homogeneous solution, the mixture was cooled down to room temperature, and then followed by adding the mixture of 5 mL of methanol solution containing NaOH (2.5 mmol) and NH<sub>4</sub>F (2.75 mmol) quickly. The reaction temperature was increased to 50 °C and the mixture was kept at this temperature for 30 min. To evaporate methanol, the reaction mixture was heated for 2 h at 120 °C. Then, the obtained mixture was further heated for 2 h at 310 °C in an argon gas atmosphere. After that, it was cooled to room temperature. The resulting NPs were precipitated by adding ethanol, collected by centrifugation, and washed three times with cyclohexane/ethanol (1:1 v/v). The obtained product was dried overnight in a vacuum oven at 50 °C.

**Modification of PVP on UCNPs.** 20 mg of UCNPs were dispersed in 20 mL of chloroform under ultrasonic treatment. Afterwards, a solution of PVP (0.4 g,  $M_w=40,000$ ) in chloroform (4 mL) was added into the UCNPs suspension, and then the mixture was stirred for 24 h at room temperature. After that, the PVP-stabilized UCNPs were precipitated with moderate hexane and collected by centrifugation at 12,000 rpm for 10 minutes. Finally, the product was washed with a mixture of chloroform and hexane several times to remove the excess free PVP and then dried overnight in a vacuum oven at 40 °C. As the main part of NaYF<sub>4</sub>:Yb/Er NPs have no change just except the capped ligand changing from oleate to PVP, we still denote the product as UCNPs in order to give a view of the NPs succinctly.

**One-Pot Synthesis of UCNPs/MB@ZIF-8.** The nanocomposite UCNPs/MB@ZIF-8 was assembled by the one-pot synthesis method referring to the reference.<sup>s2</sup> A slightly modified procedure was used. Typically, 2 mL solution of PVP-stabilized UCNPs (10 mg/mL), 2 mL solution of methylene blue (MB, 5 mg/mL), 5 mL solution of 2-methylimidazole (0.8 mol/L), and 5 mL solution of Zn(NO<sub>3</sub>)<sub>2</sub>·6H<sub>2</sub>O (0.1 mol/L) were mixed and then allowed to react at room temperature for 6 h in the dark without stirring. Methanol was used as solvent in all solution in this procedure. After that, the product was collected by centrifugation, washed several times with methanol and finally dried overnight in a vacuum oven. The obtained blue product was denoted as UCNPs/MB@ZIF-8. The molar ratio of MB:Zn<sup>2+</sup> is 1.7:100.

**Synthesis of UCNPs@ZIF-8.** UCNPs@ZIF-8 was obtained by using the same method mentioned above with the encapsulated UCNPs instead of UCNPs and MB.

**Synthesis of MB@ZIF-8.** MB@ZIF-8 was obtained by using the same method mentioned above with the encapsulated MB instead of UCNPs and MB.

**Synthesis of NH<sub>2</sub>-Modified UCNPs/MB@ZIF-8.** In order to synthesize the amino-modified UCNPs/MB@ZIF-8, we firstly stabilize a layer of PVP on the surface of UCNPs/MB@ZIF-8 to improve its hydrophilic property. Typically, 20 mg of UCNPs/MB@ZIF-8 was dispersed in 20 mL of ethanol, and then a solution of PVP (0.4 g) in ethanol (4 mL) was added into the suspension. The mixture was stirred for 18 h at room temperature, and then 5 mL of 10% (v/v) ethanolic solution of APTES was added into the above suspension slowly. The reaction was continued for another 4 h. After centrifuged at 12,000 rpm for 5 minutes and washed with ethanol several times, the obtained NH<sub>2</sub>-modified UCNPs/MB@ZIF-8 was dried in vacuum oven at 40 °C in the dark overnight. We still denote this product as UCNPs/MB@ZIF-8 to give a direct review.

**Synthesis of NH<sub>2</sub>-Modified UCNPs@ZIF-8.** NH<sub>2</sub>-modified UCNPs@ZIF-8 were obtained by using the similar method mentioned above as prepared the NH<sub>2</sub>-modified UCNPs/MB@ZIF-8 by using UCNPs@ZIF-8 in the procedure instead of UCNPs/MB@ZIF-8.

**Synthesis of NH<sub>2</sub>-Modified MB@ZIF-8.** NH<sub>2</sub>-modified MB@ZIF-8 were obtained by using the similar method mentioned above as prepared NH<sub>2</sub>-modified UCNPs/MB@ZIF-8 by using MB@ZIF-8 in the procedure instead of UCNPs/MB@ZIF-8.

**Synthesis of the Nanocomposite UCNPs/MB@ZIF-8@catalase.** 20 mg of EDC·HCl were added into a solution of 5 mL catalase (4 mg/mL, deionized water was used as the solvent in this procedure, and the pH value is 6.04), and then stirred at room temperature for 4 h to activate the carboxyl groups. Then 10 mg of NH<sub>2</sub>-modified UCNPs/MB@ZIF-8 that dispersed in 2 mL deionized water (5 mg/mL) was added into the mixture and kept stirring for 24 h in dark at room temperature. In this

process, EDC·HCl firstly conjugated with carboxyl groups to avoid influence of surroundings, and meanwhile act as a stabilizer. Thus, the reaction between carboxyl groups and NH<sub>2</sub>-modified UCNPs/MB@ZIF-8 will become simple as EDC·HCl can be easily replaced by amino groups. Finally, the product was centrifuged, washed with water three times and then freeze dried to give UCNPs/MB@ZIF-8@catalase.

**Synthesis of UCNPs@ZIF-8@catalase.** UCNPs@ZIF-8@catalase was prepared by using the similar method as UCNPs/MB@ZIF-8@catalase by using NH<sub>2</sub>-modified UCNPs@ZIF-8 instead of NH<sub>2</sub>-modified UCNPs/MB@ZIF-8. Then the following procedure is the same.

**Synthesis of MB@ZIF-8@catalase.** MB@ZIF-8@catalase was prepared by using the similar method as UCNPs/MB@ZIF-8@catalase by using NH<sub>2</sub>-modified MB@ZIF-8 instead of NH<sub>2</sub>-modified UCNPs/MB@ZIF-8. Then the following procedure is the same.

### 1.3 Experimental Methods

**Cell Culture.** Pancreatic cancer cell lines (PL 45) were provided by Hunan University (China). Cells were cultured in a regular growth medium consisting of DMEM//F12 supplemented with 10% FBS (fetal bovine serum) at 37°C in a humidified 5% CO<sub>2</sub> incubator. The cells were routinely harvested by treatment with a trypsin-ethylenediaminetetraacetic acid (EDTA) solution (0.25 %).

**Cell Cytotoxicity Assays.** To access the in-vitro cytotoxicity of different materials, the standard MTT assay was conducted on PL 45 cells. Briefly, the PL 45 cells were firstly seeded in 96-well plates at a density of 1×10<sup>5</sup> cells per well, and then cultured in 5% CO<sub>2</sub> at 37 °C for 24 h. Afterwards, free MB, UCNPs/MB@ZIF-8, UCNPs@ZIF-8@catalase and UCNPs/MB@ZIF-8@catalase were added into the cultured cells at various concentrations that were predetermined with and without 980

nm irradiation for 3 min. The cells were incubated in 5% CO<sub>2</sub> at 37 °C for another 24 h. On the other hand, cells were also cultured under an atmosphere of low oxygen content to measure the cell cytotoxicity in hypoxic cells. And then free MB, UCNPs/MB@ZIF-8, UCNPs@ZIF-8@catalase, and UCNPs/MB@ZIF-8@catalase were added into the cultured cells with 980 nm irradiation for 3 min. After that, the cells were cultured in 5% CO<sub>2</sub> at 37°C for another 24 h. Subsequently, the medium was removed and washed with fresh culturing medium. Followed by treating with 100 μL MTT (0.5 mg/mL) and incubated for another 4 h at the same conditions. Finally, the supernatant was removed, and 100 μL of dimethyl sulfoxide (DMSO) was added into the cells per well. Then the absorbance was monitored by using a microplate reader (Bio-TekELx800) at the wavelength of 580 nm. The cytotoxicity was expressed as the percentage of cell viability compared with the untreated control cells.

**Extracellular and Intracellular Detection of Singlet Oxygen.** A DPBF probe was used to measure the generation of extracellular singlet oxygen. Briefly, 150 μL of ethanol solution containing DPBF (1.0 μM) was added to 2 mL of UCNPs/MB@ZIF-8@catalase solution that dispersed in ethanol ([MB] = 20 μg/mL), and then the mixture was kept in the dark under stirring and irradiated by the 980 nm laser at various time periods. Then, the supernatant was collected for the UV–vis detection at 410 nm. The effects of 980 nm light irradiation alone, MB@ZIF-8@catalase, and UCNPs@ZIF-8@catalase samples were also investigated by the same process as UCNPs/MB@ZIF-8@catalase.

A non-fluorescent DCFH-DA probe, which could be oxidized to a highly fluorescent DCF by reactive oxygen species such as singlet oxygen, was chosen in our experiment to detect the intracellular generation of singlet oxygen. Briefly, after incubation of the PL 45 cells in the dark with 100 μg/mL UCNPs/MB@ZIF-

8@catalase, UCNPs/MB@ZIF-8, free MB and PBS for 1 h, non-internalized nanocomposites were washed with PBS, and then fresh culture medium containing DCFH-DA (10  $\mu$ M) was added for additional 1 h incubation at the same conditions. The PL 45 cells were then irradiated with the 980 nm light (1 W/cm<sup>2</sup>) for 5 min. After that, the culture medium was replaced with PBS and the fluorescence images of treated cells were acquired by using a confocal microscope. For DCF detection, the excitation wavelength was 485 nm, and the emission wavelength was 525 nm.

**Cell Death Imaging.** To study the effect of PDT, LIVE-DEAD Kits were applied to visualize cell death. Firstly, the PL 45 cells were cultured in a 96-well microplates with 100  $\mu$ L of medium at a density of  $1 \times 10^5$  cells per well, and then cultured in 5% CO<sub>2</sub> at 37 °C for 24 h. After the cells were washed, 100  $\mu$ g/mL UCNPs/MB@ZIF-8@catalase, UCNPs/MB@ZIF-8, free MB and PBS were added into the wells, and then the cells were incubated for 1 h at the same conditions. The PL 45 cells were then irradiated with the 980 nm light (1 W/cm<sup>2</sup>) for 5 min. The culture media was replaced with fresh media. After being rinsed carefully, cells were stained by LIVE-DEAD Kits for 20 min. Then the fluorescence images of treated cells were acquired by using a confocal microscope. Live cells showed green color (excitation wavelength was 488 nm), and dead cells exhibited red color (excitation wavelength was 543 nm).

**In-vitro Fluorescence Microscopy Images.** The PL 45 cell lines were incubated for 24 h, and then treated with the as-prepared UCNPs/MB@ZIF-8@catalase (200  $\mu$ g/mL) at 37°C for 0.5, 1, and 3 h, respectively. After that, the cells were washed with PBS, fixed with 2.5% formaldehyde at 37 °C for 10 min, and then washed with PBS again. The fixed cells finally immersed in 0.5 mL of PBS for the analysis. All images were collected by confocal laser scanning microscopy (CLSM, Olympus FV1000) under 980 nm.

## 2. Characterization Section

### 2.1 Dynamic Light Scattering (DLS)

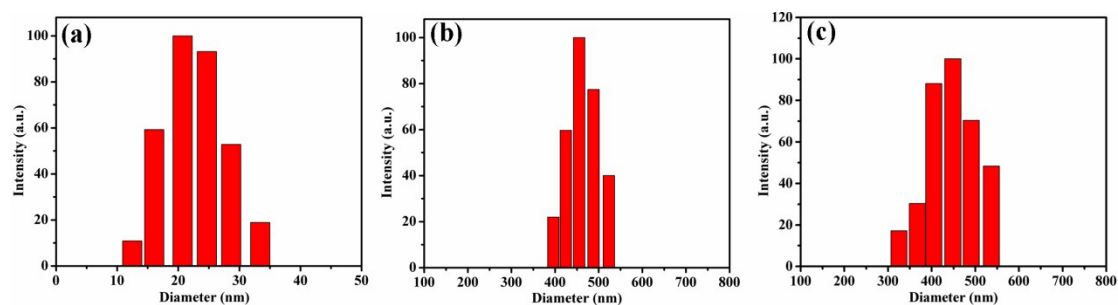


**Figure S1.** Dynamic light scattering (DLS) analysis of (a) NaYF<sub>4</sub>:Yb/Er, (b) Pure ZIF-8, and (c) UCNPs/MB@ZIF-8.

### 2.2. TEM Image of PVP-stabilized UCNPs

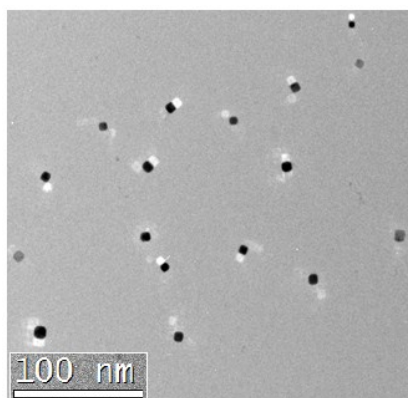


**Figure S2.** TEM image of PVP-stabilized NaYF<sub>4</sub>:Yb/Er.

### 2.3. TEM Image of UCNPs/MB@ZIF-8 (oleate-capped UCNPs)

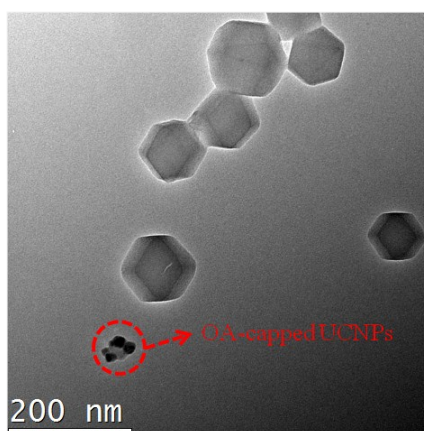


**Figure S3.** TEM image of UCNPs/MB@ZIF-8 (oleate-capped UCNPs).

## 2.4. Elemental Mapping Images of UCNPs/MB@ZIF-8

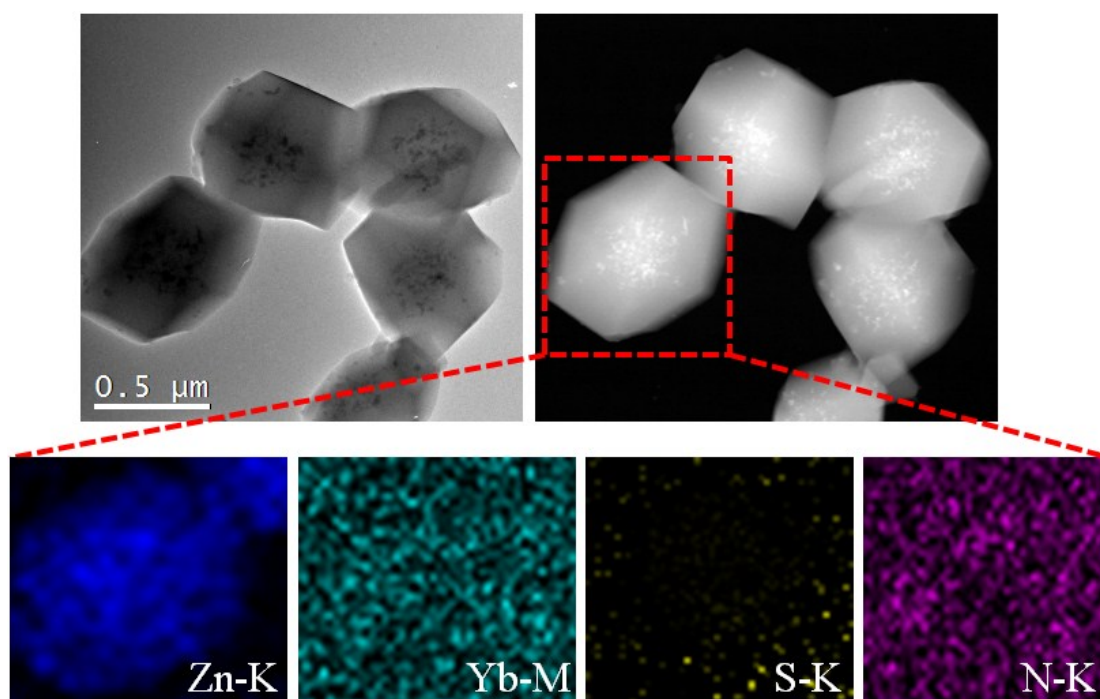


**Figure S4.** Elemental Mapping Images of UCNPs/MB@ZIF-8.

## 2.5 EDS of UCNPs@ZIF-8 and UCNPs/MB@ZIF-8

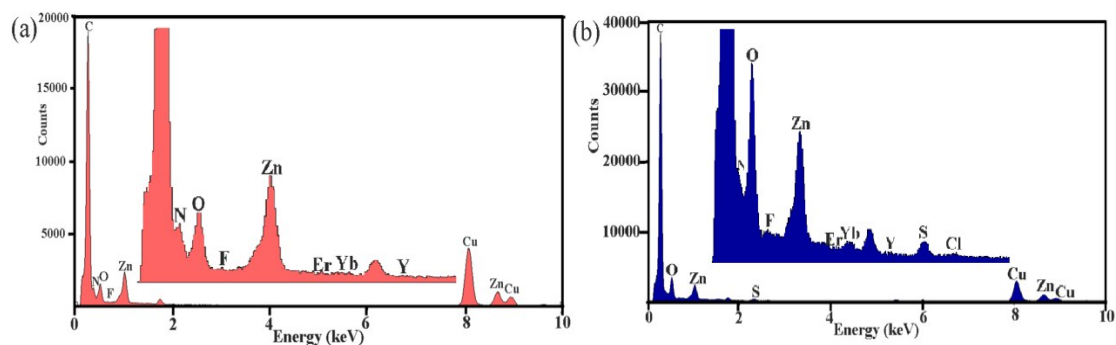


**Figure S5.** EDS of (a) UCNPs@ZIF-8 and (b) UCNPs/MB@ZIF-8 (inset: the enlarged area of EDS from 0 keV to 3 keV).

Compared with the EDS of UCNPs@ZIF-8, UCNPs/MB@ZIF-8 shows the characteristic peaks of S element and Cl element in MB molecule, which demonstrates the successful fabrication of UCNPs/MB@ZIF-8.

## 2.6. Powder X-ray Diffraction (XRD) Patterns and N<sub>2</sub> Adsorption-desorption Isotherms

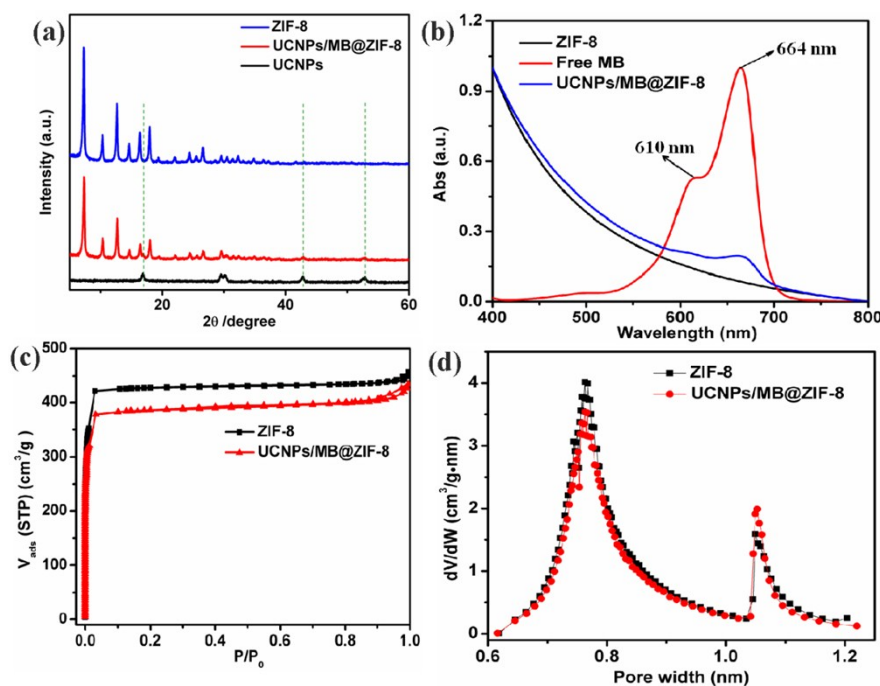


**Figure S6.** (a) PXRD patterns of ZIF-8, UCNPs and UCNPs/MB@ZIF-8, (b) UV-vis spectra of MB, ZIF-8 and UCNPs/MB@ZIF-8, (c) N<sub>2</sub> adsorption-desorption isotherms of ZIF-8 and UCNPs/MB@ZIF-8, (d) Corresponding pore-size distributions calculated by the Horvath–Kawazoe method.

Compared to the parent ZIF-8, UCNPs/MB@ZIF-8 shows the characteristic absorption peaks of MB at ~ 610 nm and ~ 664 nm (assigned to the dimers and monomers of MB, respectively, Figure S6b), which demonstrates the successful loading of MB.

ZIF-8 is a type of zeolite-like MOF and contains intersecting three-dimensional pore structures with large size (the diameter of cage and six-ring pore is 11.6 Å and 3.4 Å, respectively) and large surface area.<sup>S3</sup> As shown in Figure S6c, both samples show a type I adsorption-desorption isotherm curve behavior. The Langmuir and BET surface area for ZIF-8 are 1873 m<sup>2</sup>/g and 1367 m<sup>2</sup>/g, respectively. While for UCNPs/MB@ZIF-8, an appreciable decrease in surface area (1694 m<sup>2</sup>/g and 1241 m<sup>2</sup>/g, respectively) was observed, which can be attributed to the occupation of the cavities by UCNPs and MB molecules in the host framework; this occupation can be further demonstrated by the decrease of t-plot (t-plot typically was used to calculate the pore volume) micropore area from 1326 m<sup>2</sup>/g for ZIF-8 to 1176 m<sup>2</sup>/g for UCNPs/MB@ZIF-8. And Figure S6d shows the corresponding pore size distribution in Figure S6c.

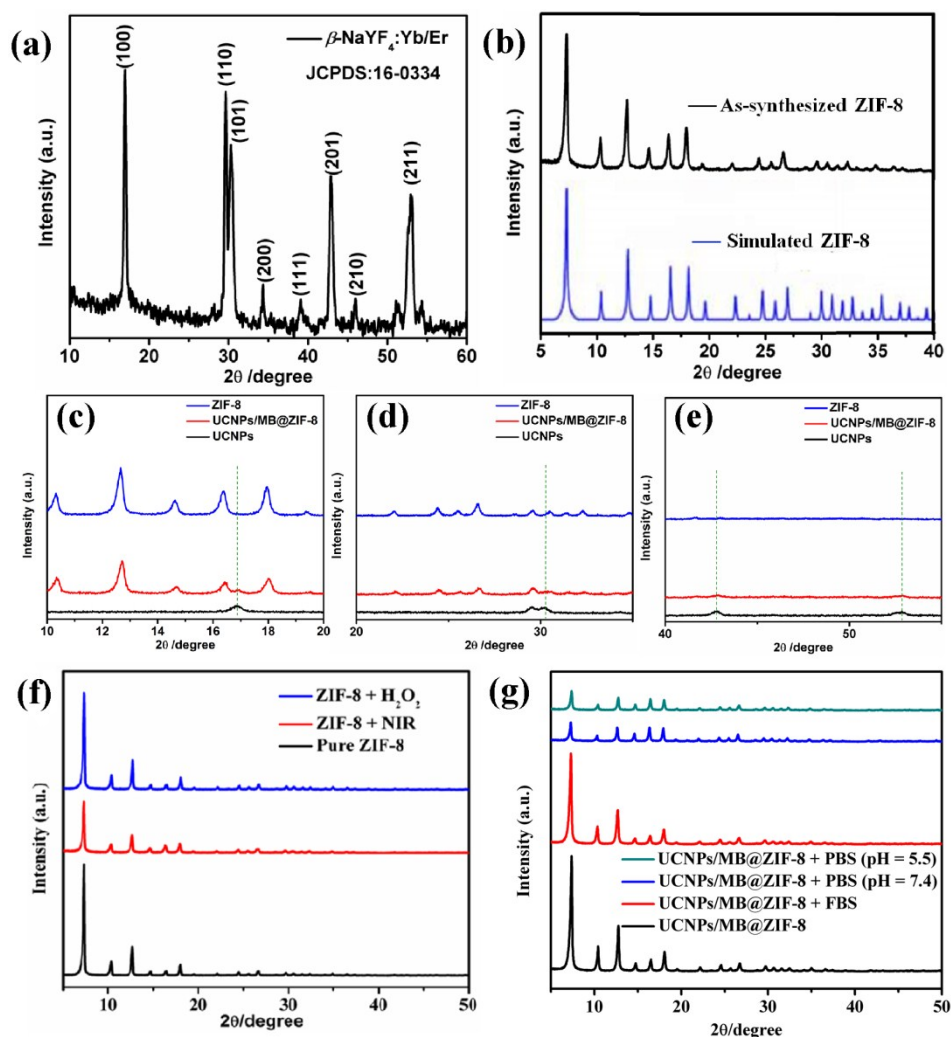


**Figure S7.** Powder X-ray Diffraction (XRD) Patterns of (a)  $\beta$ -NaYF<sub>4</sub>:Yb/Er, (b) Simulated ZIF-8 (blue line) and as-synthesized ZIF-8 (black line), (c) (d) and (e) The adjusted  $2\theta$  area of Figure 3a ranging from 10 to 20°, 20 to 35°, 40 to 55°, respectively, (f) ZIF-8 treated with 2 mL dilute H<sub>2</sub>O<sub>2</sub> solution ( $V_{\text{H}_2\text{O}_2}:V_{\text{ethanol}}=1:100$ ) for 24 h and exposed to 980 nm ( $1.5 \text{ W/cm}^2$ ) for 5 min, (g) UCNP/MB@ZIF-8 treated with fetal bovine serum (FBS) and PBS solution (two different pH value: 5.5 and 7.4) for 24 h at room temperature.

As shown in Figure S7f, the structure for ZIF-8 that treated with different conditions has almost stayed the same with pure ZIF-8, which demonstrates the stability of ZIF-8. This is important for our system. On the other hand, we also measured the stability of UCNP/MB@ZIF-8 that dispersed in FBS and PBS solution with different pH values for 24 h (Figure S7g). It can be seen clearly that the structure of UCNP/MB@ZIF-8 only has little change compared to that without treatment, especially when dispersed in FBS. We believe it a reasonable design and will provide a new pathway for the future PDT.

## 2.7. Elemental Mapping Images and XPS of UCNPs/MB@ZIF-8@catalase

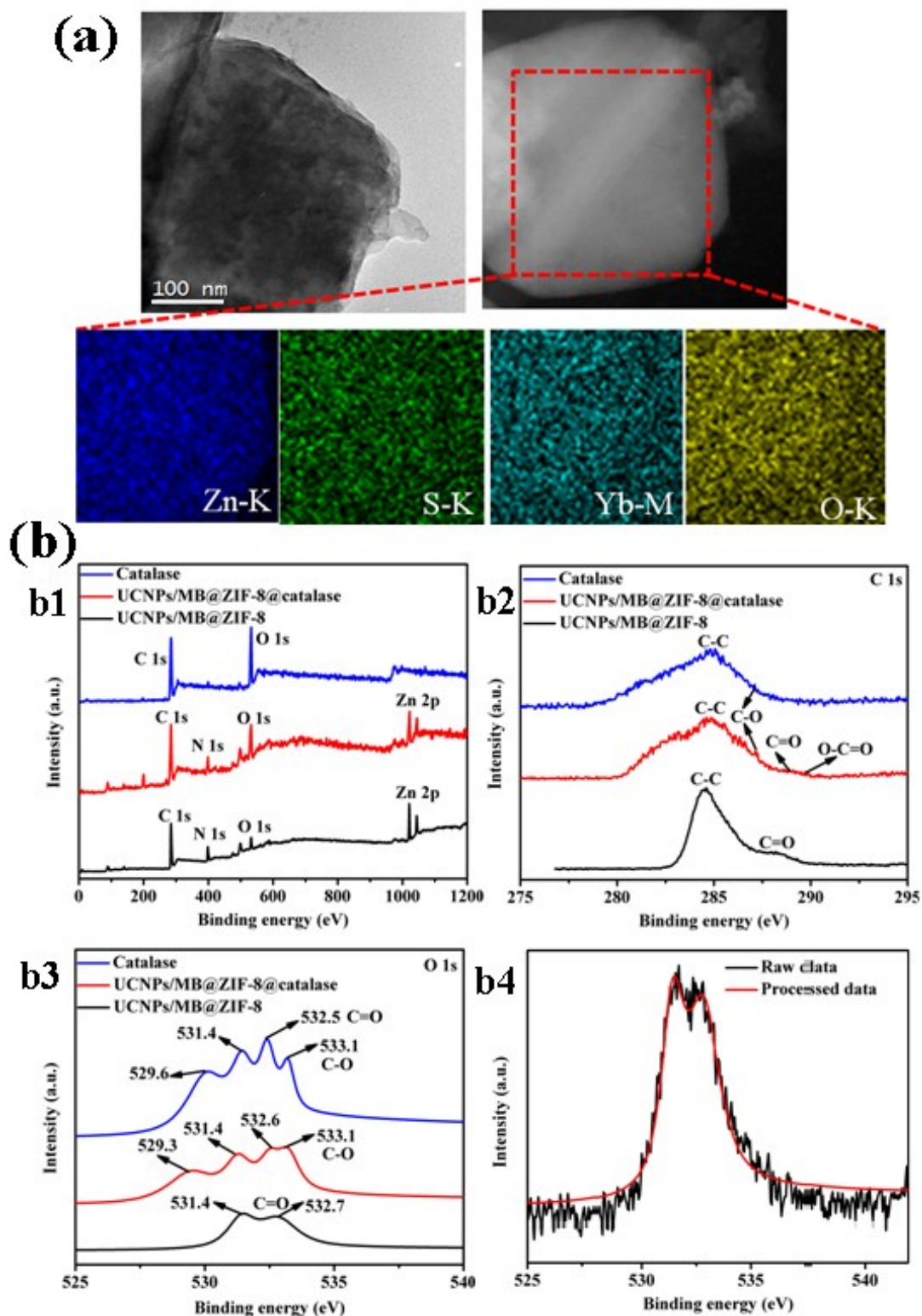


**Figure S8.** Elemental mapping images (a) and XPS (b) of UCNPs/MB@ZIF-8@catalase (The binding energies in XPS are referred to C 1s (284.6 eV)).

As shown in Figure S8(a), the edge of UCNPs/MB@ZIF-8@catalase becomes blurred and a thick shell appears compared with UCNPs/MB@ZIF-8 (Figure S4), and

oxygen can be found in the elemental mapping, which demonstrate the successful conjugation of catalase on the surface of ZIF-8. On the other hand, we also measured XPS of different materials (Figure S8b). It can be seen that C 1s, N 1s, O 1s and Zn 2p all exist in UCNPs/MB@ZIF-8 and UCNPs/MB@ZIF-8@catalase while only C 1s and O 1s can be found in catalase (b1). From the high-resolution XPS of C 1s (b2), Two peaks at around 284.6 eV and 288.1 eV can be found in UCNPs/MB@ZIF-8, which can be attributed to C-C and C=O of PVP on the surface of ZIF-8, respectively.<sup>S4</sup> But for UCNPs/MB@ZIF-8@catalase, two new peaks at around 286.3 eV and 289.1 eV appear, which can be assigned to C-O and O-C=O (-COOH) coming from catalase.<sup>S4</sup> Moreover, peaks at 531.4 eV and 532.7 eV of O 1s correspond to C=O of PVP<sup>S4b</sup> and adsorbed water molecules<sup>S5</sup> (b3). However, new peaks at 533.1 eV and 529.3 eV which are attributed to C-O<sup>S4b</sup> and chemisorbed surface oxygen<sup>S6</sup> can be another proofs that demonstrate the successful conjugation of catalase. (b4 is one of the examples in b3 where raw data were slightly smoothed in XPSPEAK41. The result is so near to the raw data that we can use the processed data directly.)

### 3. Spectroscopic Studies

#### 3.1. UV-vis Spectra

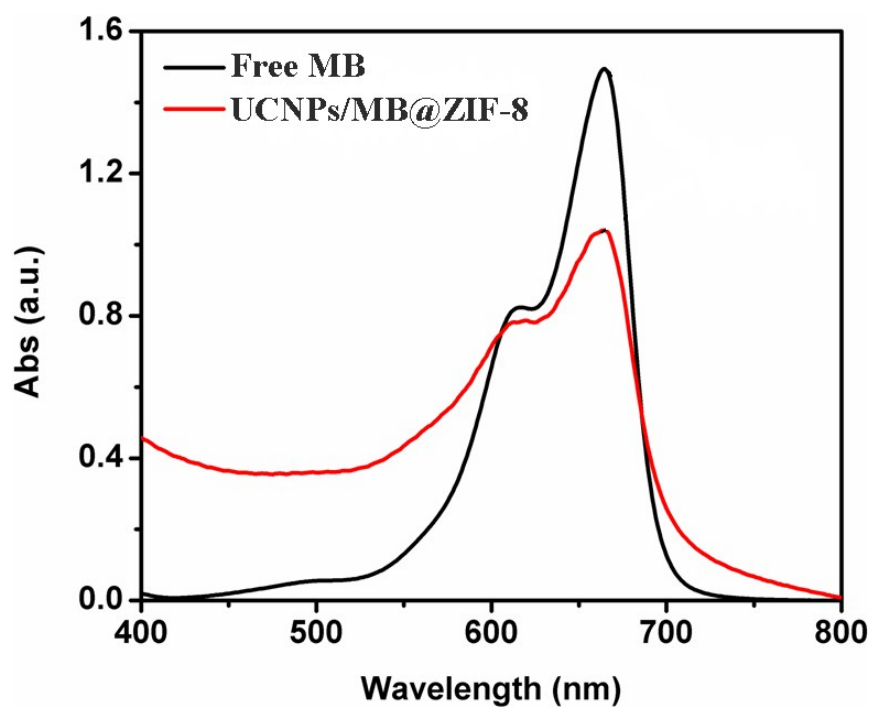


Figure S9. UV-vis spectra of free MB and UCNPs/MB@ZIF-8.

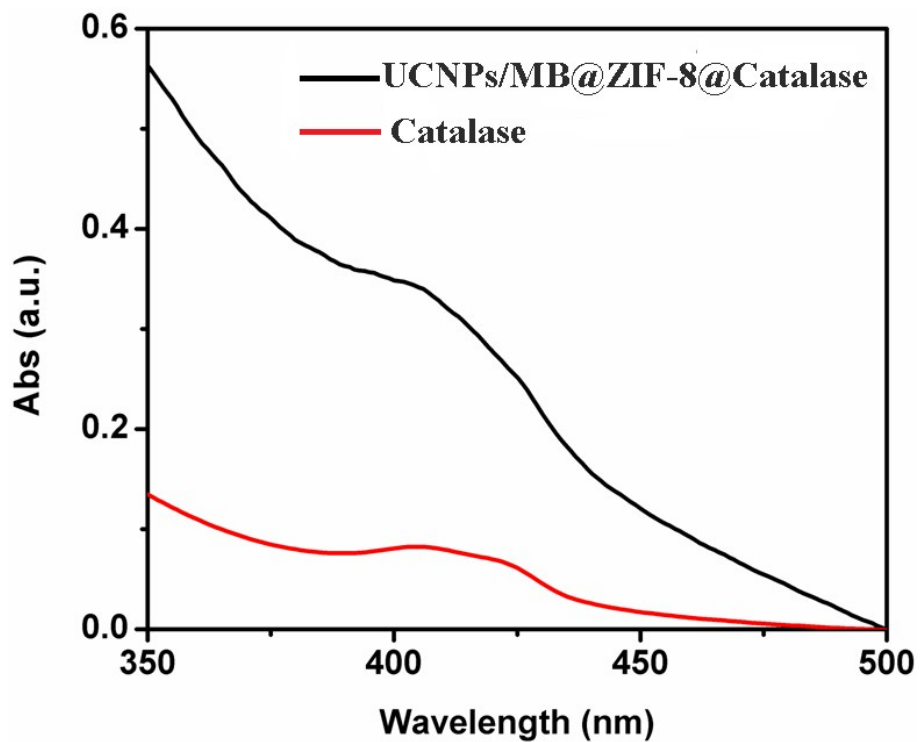
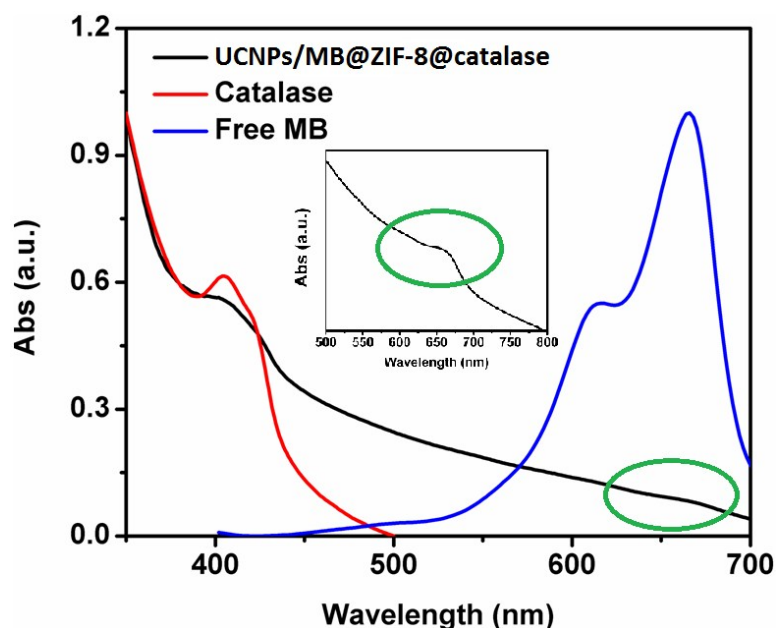
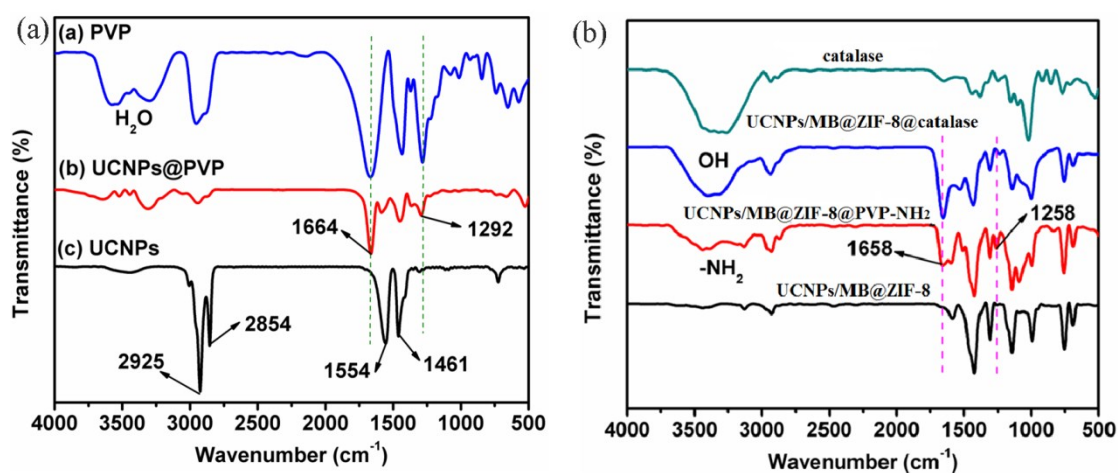


Figure S10. UV-vis spectra of catalase and UCNPs/MB@ZIF-8@catalase.



**Figure S11.** UV-vis spectra of catalase, free MB and UCNPs/MB@ZIF-8@catalase.

### 3.2. FTIR Spectra



**Figure S12.** (a) FTIR spectra of OA-stabilized NaYF<sub>4</sub>:Yb/Er, PVP-stabilized NaYF<sub>4</sub>:Yb/Er and PVP. (b) FTIR spectra of UCNPs/MB@ZIF-8, UCNPs/MB@ZIF-8@PVP-NH<sub>2</sub>, UCNPs/MB@ZIF-8@catalase, and catalase.

As shown in figure S9a, the FTIR spectrum of OA-UCNPs exhibits the carboxylate stretching at 1554 cm<sup>-1</sup> and 1461 cm<sup>-1</sup>. The absorption bands at 2925 cm<sup>-1</sup>, 2854 cm<sup>-1</sup> are assigned to -CH<sub>2</sub> (ν<sub>as</sub>), -CH<sub>2</sub> (ν<sub>a</sub>), respectively. These indicate the successful synthesis of the OA-capped UCNPs. After the ligand OA is exchanged by PVP, it shows a strong carbonyl stretching (C=O) peak at 1664 cm<sup>-1</sup> and a characteristic stretching (C-N) peak at 1292cm<sup>-1</sup>, which demonstrate the successful exchange of OA

with PVP. In addition, the broad absorption band at about  $3500\text{cm}^{-1}$  is due to the adsorbent water molecules.

Compared with UCNPs/MB@ZIF-8 (Figure S12b), the FTIR spectrum of UCNPs/MB@ZIF-8@PVP-NH<sub>2</sub> shows a strong carbonyl stretching (C=O) peak at  $1658\text{ cm}^{-1}$ , which is due to the polymer PVP. The broad absorption band from  $3300\text{ cm}^{-1}$  to  $3500\text{ cm}^{-1}$  is assigned to the amino groups, which demonstrates the successful modification of NH<sub>2</sub> on UCNPs/MB@ZIF-8@PVP. For UCNPs/MB@ZIF-8@catalase, the broad absorption band around  $3500\text{ cm}^{-1}$  is due to the -OH groups in catalase, which demonstrates the successful conjugation of catalase on UCNPs/MB@ZIF-8.

### 3.3. Fluorescence Spectra

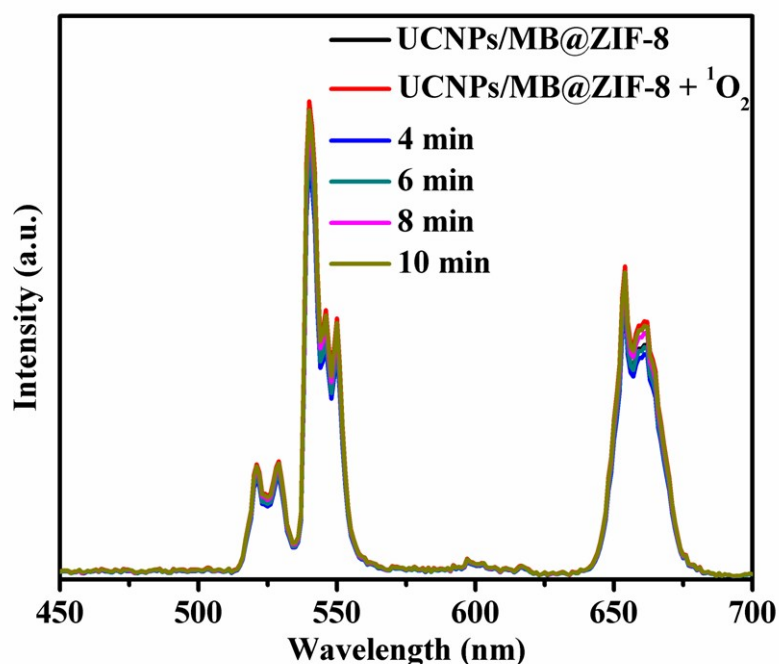


**Figure S13.** Upconverting luminescence spectra of UCNPs/MB@ZIF-8 in the presence of singlet oxygen at different time periods (the excitation wavelength is 980 nm).

#### 4. Zeta Potential

Table S1. Zeta potential of catalase, UCNPs/MB@ZIF-8@catalase, and UCNPs/MB@ZIF-8@PVP-NH<sub>2</sub>.

	UCNPs/MB@ZIF-8@PVP-NH <sub>2</sub>	UCNPs/MB@ZIF-8@catalase	catalase
<b>ζ potential</b>	<b>+42.6mV</b>	<b>+4.8mV</b>	<b>-25.6mV</b>

#### 5. The Decay Curves

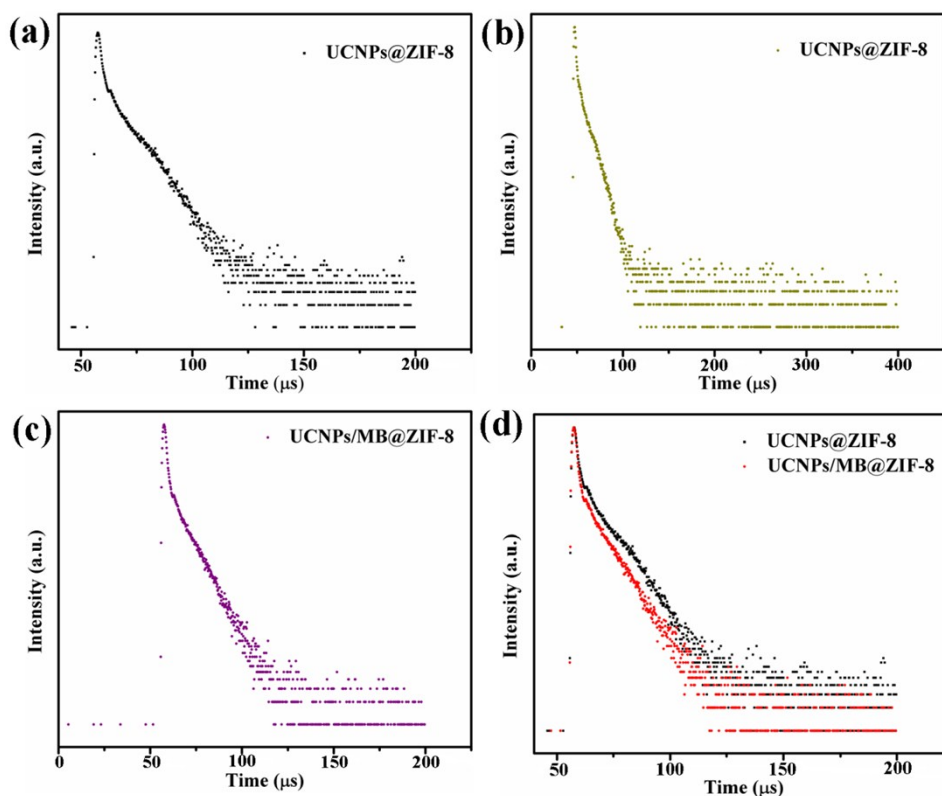


**Figure S14.** Decay curves of  $\text{Er}^{3+}$  at 654 nm in (a) and (b) UCNP@ZIF-8, (c) UCNP/MB@ZIF-8, (d) all the two decay times of UCNP@ZIF-8 and UCNP/MB@ZIF-8 (with the same time axis) in the same picture.

As shown in Figure S14, we give two decay curves of UCNP@ZIF-8 with different time axis. In order to give a direct difference between UCNP@ZIF-8 and UCNP/MB@ZIF-8, (a) was chosen to merge with (c). However, for the lifetimes, (b) is suitable to be fitted. It can be seen clearly that fluorescence of UCNP/MB@ZIF-8 decays faster than UCNP@ZIF-8, which demonstrates a FRET process between UCNP and MB.

**Table S2.** The lifetime of different materials

	$\tau_1(\mu\text{s})$	$\tau_2(\mu\text{s})$	$\langle\tau\rangle(\mu\text{s})$
UCNP@ZIF-8	10.174 (100%)	—	10.174
UCNP/MB@ZIF-8	1.539 (8.83%)	9.011 (91.17%)	8.351

## 6. The Oxygen-Generation Performance of UCNP/MB@ZIF-8@catalase

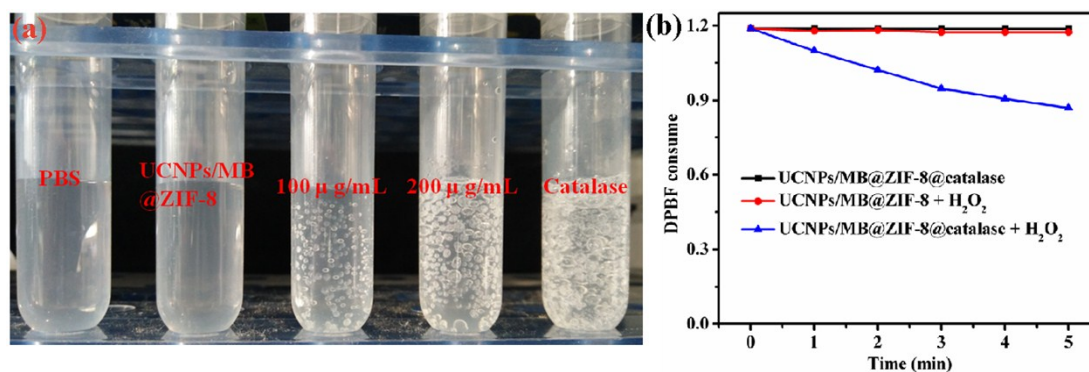


**Figure S15.** (a) Photographs of different materials (100  $\mu\text{g/mL}$  and 200  $\mu\text{g/mL}$  designate the concentrations of UCNPs/MB@ZIF-8@catalase dispersed in PBS solution) after adding dilute H<sub>2</sub>O<sub>2</sub> (2 mM). (b) Absorption of DPBF at 410 nm as a function of 980 nm (1 W/cm<sup>2</sup>) irradiation time under N<sub>2</sub> atmosphere in different conditions.

A large quantity of oxygen bubble can be observed when adding a small amount of H<sub>2</sub>O<sub>2</sub> to an UCNPs/MB@ZIF-8@catalase solution; while there is no bubble in the solution containing UCNPs/MB@ZIF-8. In addition, the quantity of oxygen bubble increases along with the increasing concentration of UCNPs/MB@ZIF-8@catalase solution, which is due to the more catalase in the system.

## 7. The Leakage of MB

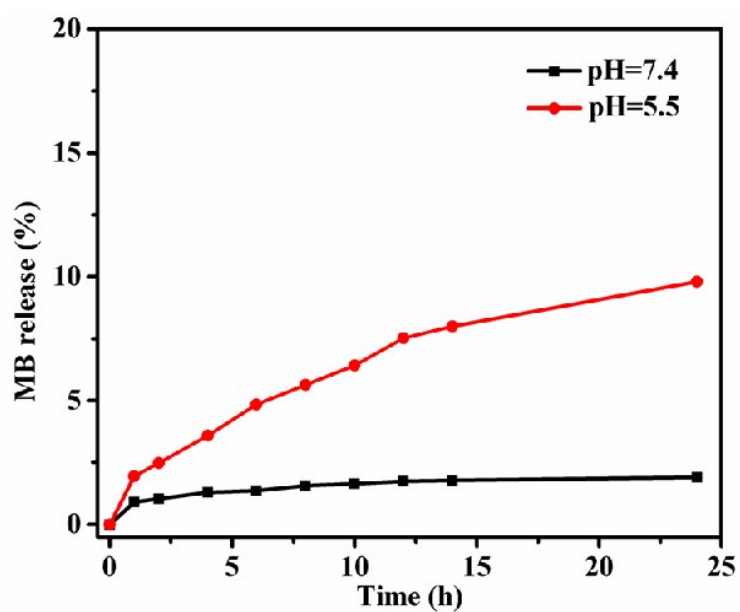


**Figure S16.** The leakage of MB in different conditions.

## 8. Cell Viability and Intracellular Generation of Singlet Oxygen

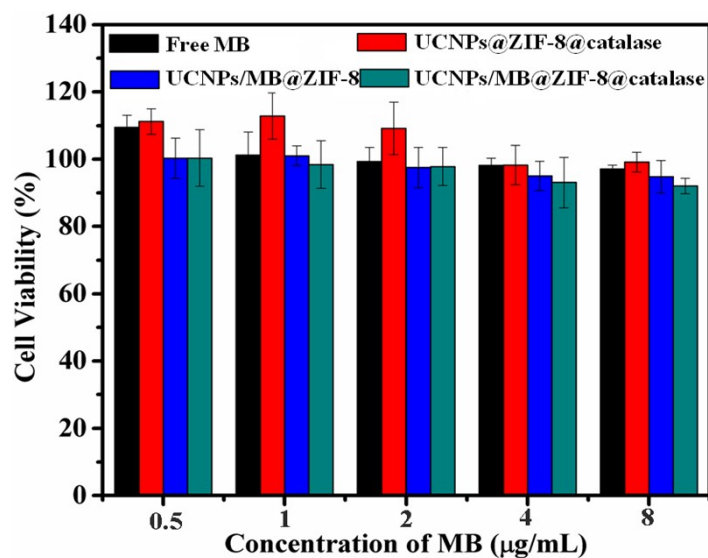


**Figure S17.** Cell viabilities that cultured with different materials in dark.

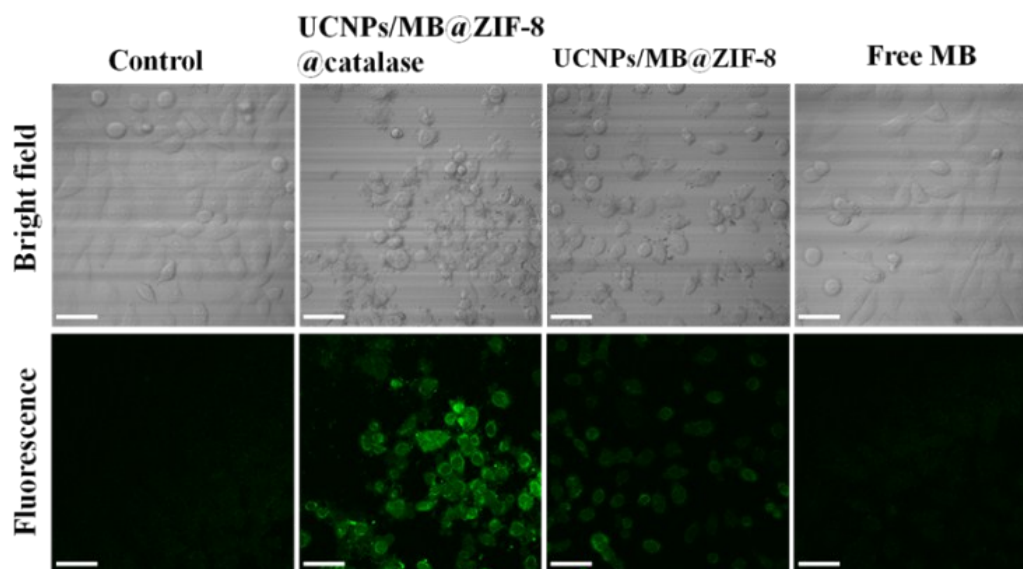


**Figure S18.** Confocal images of an intracellular singlet oxygen generation in PL45 cells incubated with UCNPs/MB@ZIF-8@catalase, UCNPs/MB@ZIF-8 or free MB after 980 nm irradiation ( $1 \text{ W/cm}^2$ ) for 5 min.

## 9. Cell Death Imaging and In-vitro Confocal Microscope Images

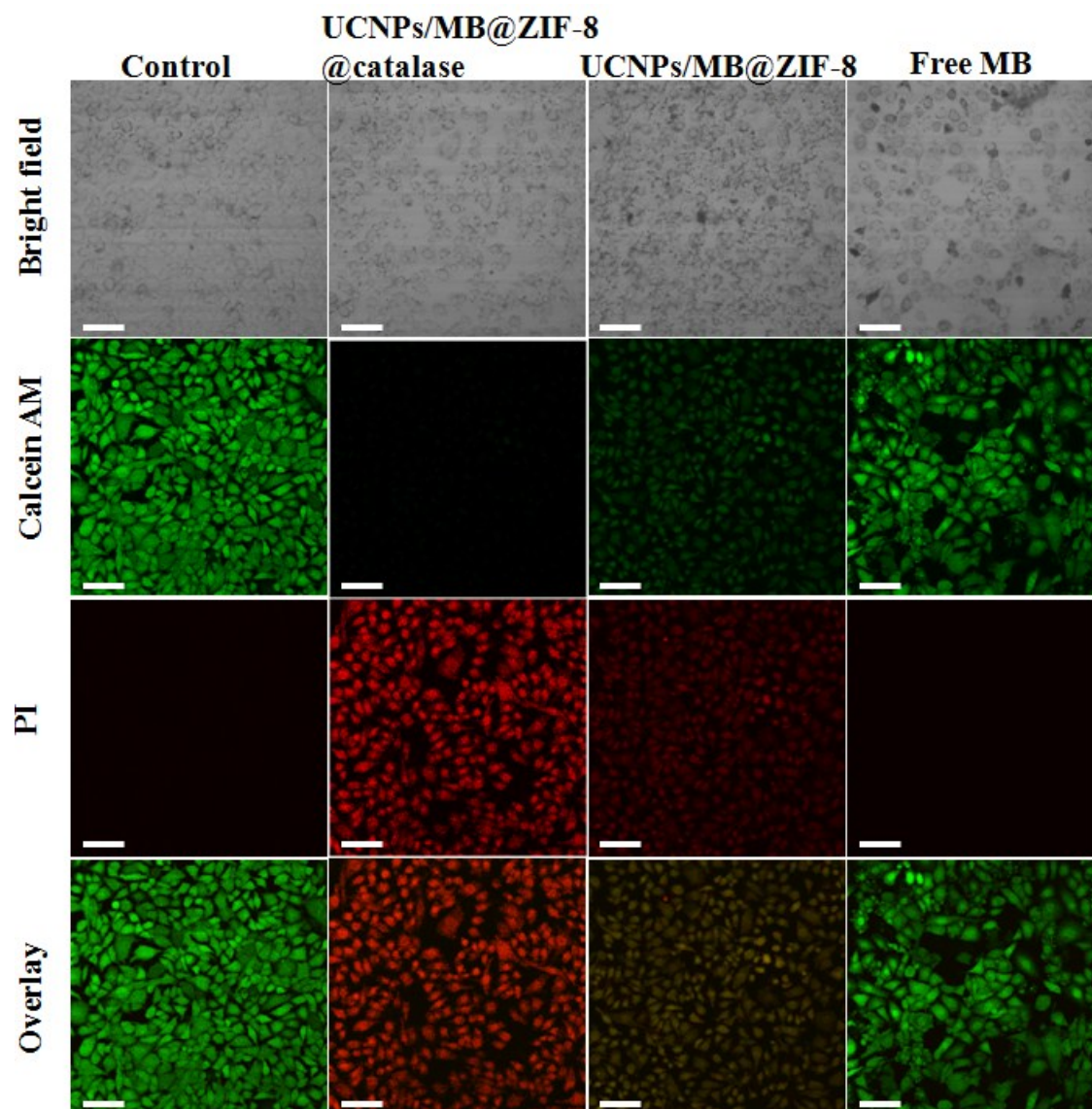


**Figure S19.** Corresponding confocal images of PL45 cells incubated with UCNPs/MB@ZIF-8@catalase, UCNPs/MB@ZIF-8 or free MB after 980 nm irradiation (1 W/cm<sup>2</sup>) for 5 min and co-stained with calcein AM (green, live cells) and propidium iodide (PI, red, dead cells) (Scale bar = 100  $\mu$ m).

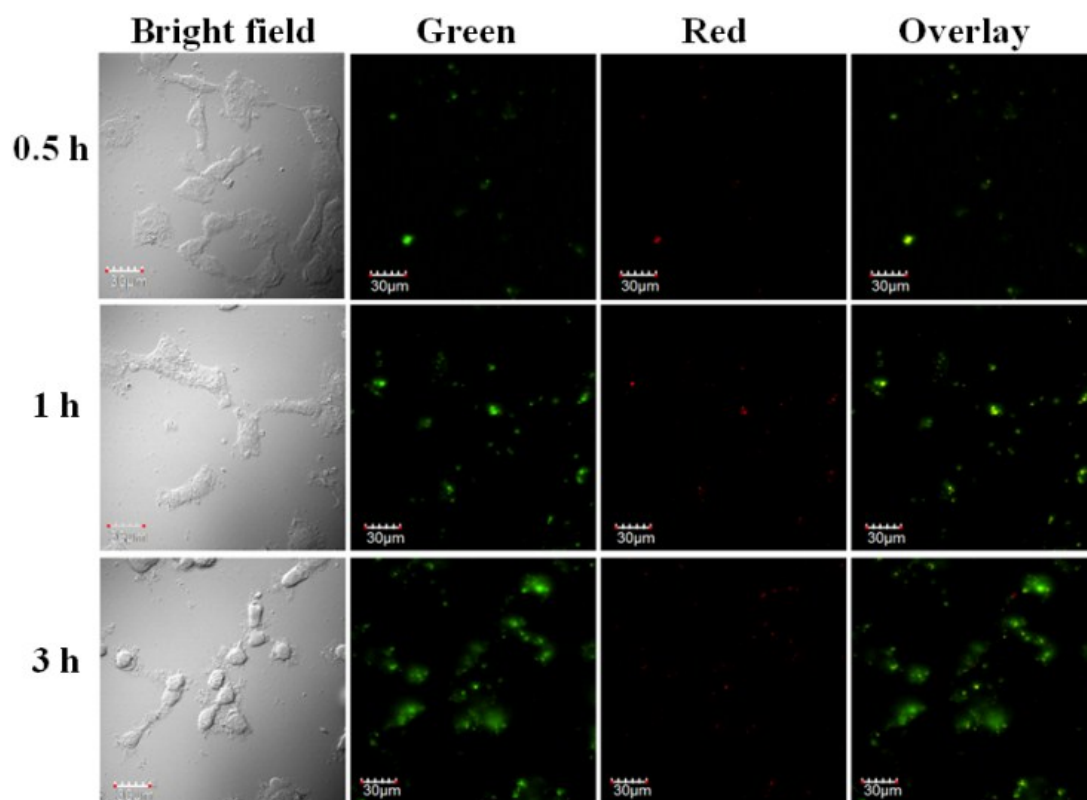


**Figure S20.** In-vitro confocal microscopy images of PL45 cells incubated with UCNPs/MB@ZIF-8@catalase for 0.5, 1, and 3 h.

## References

- [S1] Z. Q. Li, Y. Zhang, *Nanotechnology* 2008, **19**, 345606-345611.
- [S2] G. Lu, S. Z. Li, Z. Guo, O. K. Farha, B. G. Hauser, X. Y. Qi, Y. Wang, X. Wang, S. Y. Han, X. G. Liu, C. N. Du, H. Zhang, Q. C. Zhang, X. D. Chen, J. Ma, S. C. J. Loo, W. D. Wei, Y. H. Yang, J. T. Hupp, F. W. Huo, *Nature Chem.* 2012, **4**, 310-316.
- [S3] a) K. S. Park, Z. Ni, A. P. Côté, J. Y. Choi, R. Huang, F. J. Uribe-Romo, H. K. Chae, M. O’Keeffe, O. M. Yaghi, *Proc. Natl. Acad. Sci. U.S.A.* 2006, **103**, 10186-10191; b) X. C. Huang, Y. Y. Lin, J. P. Zhang, X. M. Chen, *Angew. Chem. Int. Ed.* 2006, **45**, 1557-1559.
- [S4] a) R. F. Nie, J. H. Wang, L. N. Wang, Y. Qin, P. Chen, Z. Y. Hou, *Carbon* 2012, **50**, 586-596; b) S. Zhao, B. Rasimick, W. Mustain, H. Xu, *Appl. Catal. B: Environ.* 2017, **203**, 138-145.
- [S5] L. G. Xia, J. Bai, J. H. Li, Q. Y. Zeng, L. S. Li, B. X. Zhou, *Appl. Catal. B: Environ.* 2017, **204**, 127-133.
- [S6] R. Viter, I. Iatsunskiy, V. Fedorenko, S. Tumenas, Z. Balevicius, A. Ramanavicius, S. Balme, M. Kempniński, G. Nowaczyk, S. Jurga, M. Bechelany, *J. Phys. Chem. C* 2016, **120**, 5124–5132.